

## Investigation of thermal annealing effects on the optical transparency and luminescent characteristics of Eu-doped $Y_2O_3$ thin films

Myun Hwa Chung and Joo Han Kim\*

Department of Advanced Materials Engineering, Chungbuk National University, Cheongju 28644, Korea

The thermal annealing effects on the optical transparency and luminescent characteristics of the Eu-doped  $Y_2O_3$  thin films have been investigated. The as-deposited  $Y_2O_3:Eu$  films exhibited an optical band gap of 5.78 eV with a transparency of 89 % at a wavelength of 550 nm. As the annealing temperature increased from 1000 to 1300 °C, the optical band gap and transparency of the films decreased from 5.77 to 4.91 eV and from 86.8 to 64.5 % at 550 nm, respectively. The crystalline quality of the films was improved with increasing annealing temperature. The annealed  $Y_2O_3:Eu$  films emitted a red-color photoluminescence (PL) with the highest emission peak near 612 nm. The PL intensity was increased with increasing annealing temperature to 1200 °C, resulting from the improvement in the crystalline quality of the films. The PL intensity was decreased with further increasing temperature above 1200 °C due to the formation of  $Y_2SiO_5$  phase by the reaction of the film with the quartz substrate.

**Key words:** Transparency, Optical band gap, Yttrium oxide, Thermal annealing

### Introduction

Lanthanide (Ln)-doped oxides are one of the most important class of luminescent materials which have attracted intense attention. These materials have been widely used in optical applications due to the unique luminescent features of Ln ions [1-3]. The light emission from the Ln ions originates primarily from the  $4f^n$  intrashell transitions. The partially filled  $4f$  inner shell in the Ln ions is shielded from the surroundings by the completely filled  $5s^2$  and  $5p^6$  outer shells. Therefore, the emission spectra of Ln ions generally appear as very narrow and sharp peaks at wavelengths which are weakly dependent on the coordination environment or the crystal field [3].

Among various Ln-doped oxides, europium-doped yttrium oxide ( $Y_2O_3:Eu$ ) has been intensively studied owing to its red luminescence with high efficiency and good color purity [4-6].  $Y_2O_3:Eu$  has been practically used as a red-emitting cathodoluminescent and photoluminescent material for various types of display devices, such as field emission displays (FEDs), vacuum fluorescent displays (VFDs), and plasma panel displays (PDPs) [7-10].  $Y_2O_3:Eu$  is typically prepared in powdered form by using various synthesis techniques [4-12]. Special attention also needs to be paid to thin film form of  $Y_2O_3:Eu$  because it has diverse potential

applications [13]. In particular, thin  $Y_2O_3:Eu$  films with a high transparency in the visible wavelength region could be used as a red light emission layer in transparent display devices [14]. In this study, optically transparent and luminescent thin films of  $Y_2O_3:Eu$  were deposited by radio frequency (RF) magnetron sputtering. This work primarily aimed to clarify the effects of thermal annealing treatment on the optical transparency and the luminescent characteristics of the  $Y_2O_3:Eu$  films. The relationship between the structure and luminescence of the  $Y_2O_3:Eu$  films was also examined.

### Experimental

The optically transparent  $Y_2O_3:Eu$  thin films were deposited by using an RF magnetron sputtering technique. Sputtering was carried out on fused quartz substrates using an Eu-doped  $Y_2O_3$  target in an Ar gas atmosphere. Prior to deposition of the films, the sputtering chamber was pumped by a turbomolecular pump until a base pressure of less than  $1 \times 10^{-6}$  Torr was achieved. The deposition was performed with no substrate heating. The gas pressure and the RF power density were held at  $2 \times 10^{-2}$  Torr and  $5.92 \text{ Wcm}^{-2}$ , respectively, during deposition. The film thickness was maintained at approximately 500 nm by adjusting the deposition time. The deposited films were thermally annealed for 1 hour in air ambient at temperatures from 1000 to 1300 °C.

The optical transmittance spectra of the  $Y_2O_3:Eu$  films were monitored on a Perkin Elmer Lambda 35

\*Corresponding author:  
Tel : +82-43-261-2413  
Fax: +82-43-271-3222  
E-mail: joohan@cbnu.ac.kr

spectrophotometer in the spectral range between 190 and 1100 nm. The crystalline quality of the films was analyzed by X-ray diffraction (XRD), which was performed using a SmartLab Rigaku diffractometer equipped with Cu  $K\alpha_1$  radiation. To determine the surface morphology of the films, atomic force microscopy (AFM) measurements were performed using a Bruker Dimension Icon. Photoluminescence (PL) emission and excitation spectra of the films were measured at wavelengths from 200 to 800 nm with a resolution of 0.5 nm using a xenon discharge lamp as an excitation source.

## Results and Discussion

The optical transmission spectra were measured for the  $Y_2O_3:Eu$  films and are presented in Fig. 1 with the variation of annealing temperatures. The as-deposited films exhibit an optical absorption edge in ultraviolet region and a high transparency in visible and near-infrared regions. It can be seen that the transparency is reduced as the annealing temperature increases. The as-deposited films have an optical transmittance of 89% at a wavelength of 550 nm. The transmittance reduces to 86.8% after annealing the films at 1000 °C, and then to 64.5% after annealing at 1300 °C. The optical band gap,  $E_g$  of the  $Y_2O_3:Eu$  films can be estimated using the following equation [15]:

$$(\alpha h\nu)^2 = A(h\nu - E_g) \quad (1)$$

where  $\alpha$  is the optical absorption coefficient,  $h\nu$  is the photon energy, and  $A$  is the constant. The obtained  $E_g$  values are presented in Fig. 2 as a function of annealing temperature. The  $E_g$  is found to be 5.78 eV for the as-deposited films, which is comparable with the value reported for yttrium oxide [16]. The  $E_g$  slightly decreases

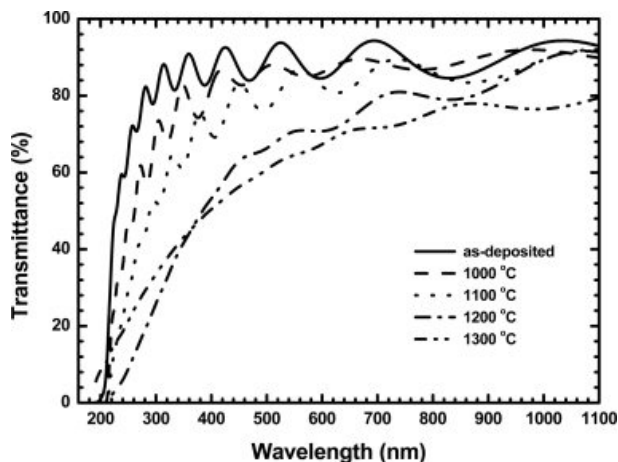


**Fig. 1.** The optical transmittance spectra obtained from the as-deposited  $Y_2O_3:Eu$  films and the films annealed at different temperatures.

as the annealing temperature increases to 1200 °C. A significant reduction in  $E_g$  for the films annealed at 1300 °C is considered to be due to the formation of  $Y_2SiO_5$  phase, as will be discussed below with the X-ray diffraction data.

Fig. 3 presents the X-ray diffraction patterns of the as-deposited  $Y_2O_3:Eu$  films and the films annealed at different temperatures. It can be found in Fig. 3(a) that the as-deposited films had a mixed structure of cubic and monoclinic  $Y_2O_3$  phases. The peaks marked with Miller indices in the pattern are those from the cubic  $Y_2O_3$  phase [17]. The peaks marked with the symbol ( $\circ$ ) correspond to the monoclinic  $Y_2O_3$  phase [18]. After annealing treatment, the XRD patterns show much more intense and narrower peaks as compared to those of the as-deposited films, indicating that the crystalline quality of the films was significantly improved by the anneal. The annealed films show the peaks from the cubic  $Y_2O_3$  phase with a preferential orientation along the (400) plane. After annealing at 1200 °C, as shown in Fig. 3(d), the diffraction peaks attributed to the  $Y_2SiO_5$  phase start to appear. The peaks marked with the symbol ( $\nabla$ ) correspond to the  $Y_2SiO_5$  phase [19]. At 1300 °C, as shown in Fig. 3(e), the diffraction pattern is dominated by the peaks from the  $Y_2SiO_5$  phase as the reaction between the film and the quartz substrate was accelerated at this high temperature. Most of the peaks, except for the (211) and (400) peaks of the cubic  $Y_2O_3$  phase, arose from the  $Y_2SiO_5$  phase. In order to analyze the crystalline quality of the films, we measured the full width at half maximum (FWHM) of the (400) peak from the cubic  $Y_2O_3$  phase. As shown in Table 1, the FWHM is  $0.5415^\circ$  for the as-deposited films and significantly reduces to  $0.2274^\circ$  by annealing at 1000 °C. The FWHM decreases with further increasing annealing temperature and reaches 0.1480 at 1300 °C. This clearly indicates the improved crystalline quality

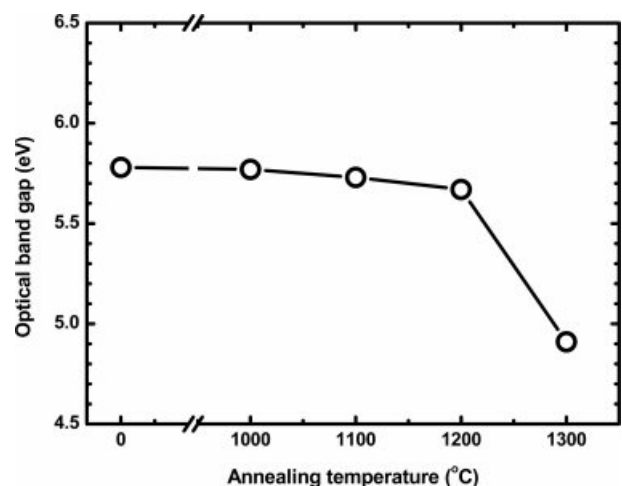


**Fig. 2.** The optical band gap as a function of the annealing temperature.

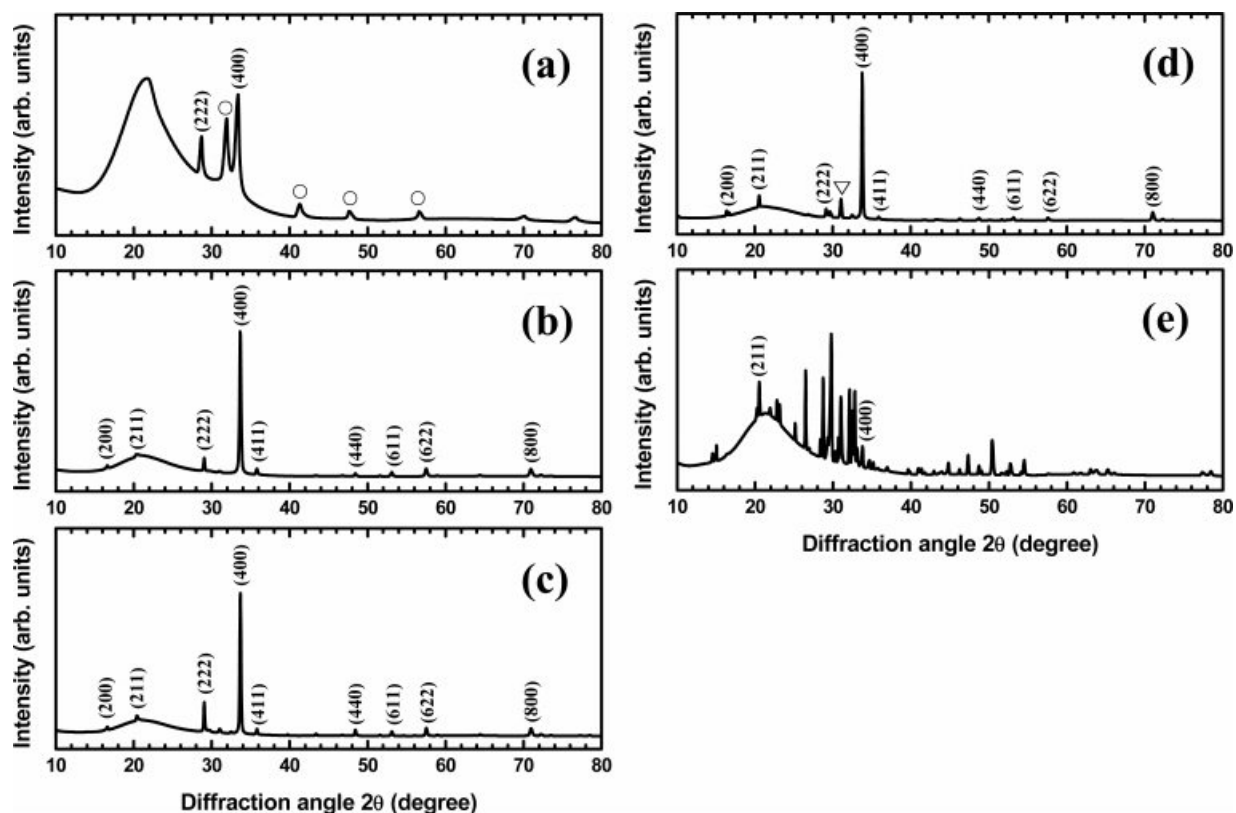


Fig. 3. XRD patterns of the  $Y_2O_3:Eu$  films (a) as-deposited and annealed at (b) 1000 °C, (c) 1100 °C, (d) 1200 °C, and (e) 1300 °C.

**Table 1.** Full width at half maximum of the (400) peak measured at different annealing temperatures.

Annealing temperature (°C)	FWHM (°)
as-deposited	0.5415
1000	0.2274
1100	0.1913
1200	0.1760
1300	0.1480

at higher annealing temperature.

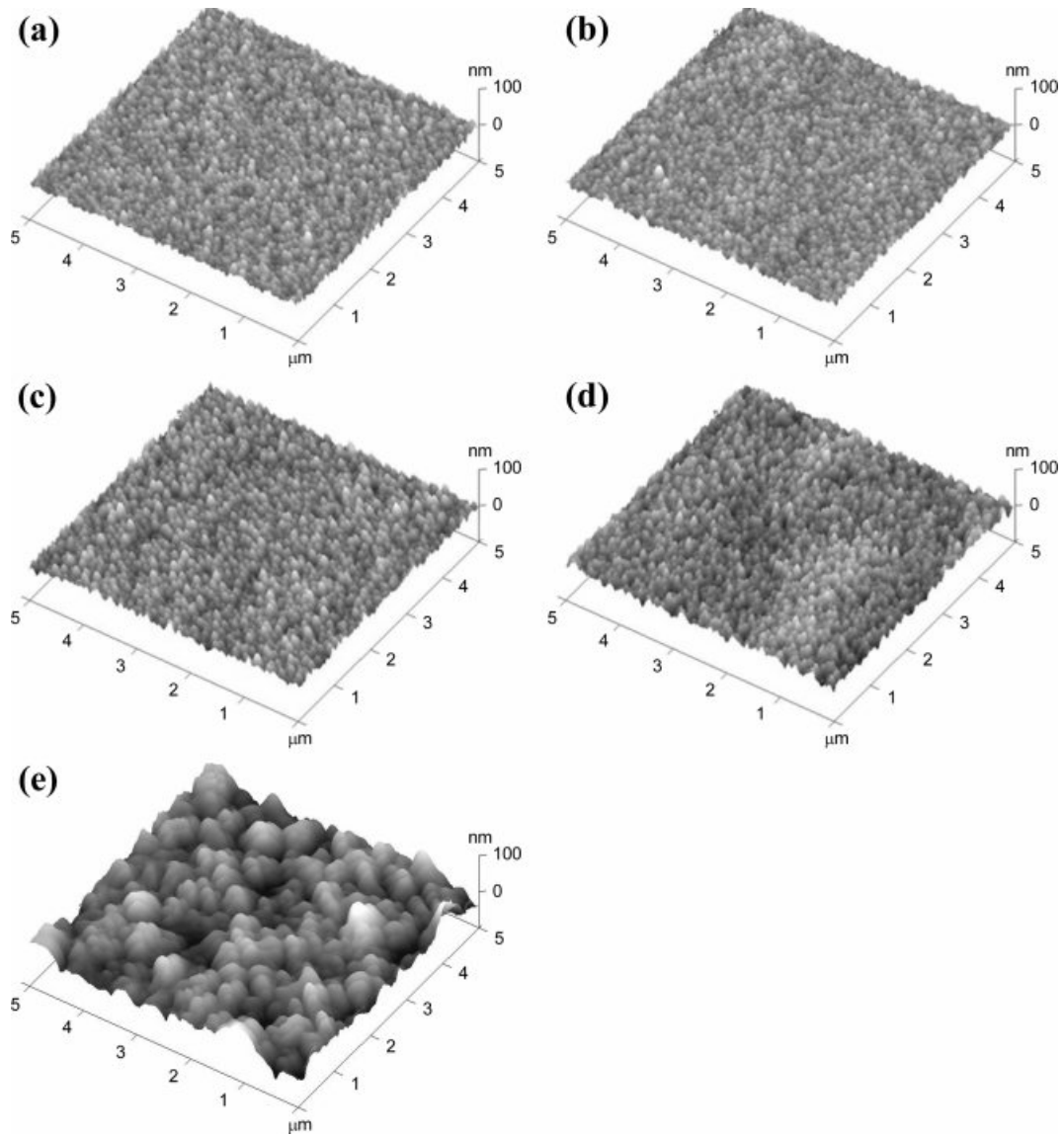
Fig. 4 shows AFM images for the as-deposited and annealed  $Y_2O_3:Eu$  films. It can be found that no obvious change in surface morphology was observed after annealing at temperatures up to 1100 °C. The surface of the films became rougher as the annealing temperature was raised above 1200 °C, resulting from the reaction between the film and the quartz substrate. It should be mentioned that cracks appeared at the surface of the samples after the annealing treatment. It is believed that the cracks were caused during annealing, probably due to the difference of the thermal expansion coefficient between the  $Y_2O_3:Eu$  film and the quartz substrate.

Fig. 5 shows the PL emission spectra of the  $Y_2O_3:Eu$  films annealed at different temperatures. The as-

deposited films did not show any PL emission because of their poor crystalline quality. As shown in Fig. 5, several PL emission peaks were detected from the annealed films, which originated from the  $f-f$  transitions of  $Eu^{3+}$  ions. These PL spectra are similar to those observed from the  $Y_2O_3:Eu$  powders [8]. The highest emission peak near 612 nm in the red range is associated with the transition from the  $^5D_0$  excited state to the  $^7F_2$  level. The PL excitation spectra of the  $Y_2O_3:Eu$  films annealed at different temperatures are shown in Fig. 6. The excitation band below 219 nm is due to the absorption of  $Y_2O_3$  host lattice. Additional bands observed in the range between 219 and 290 nm are related to the charge transfer between  $O^{2-}$  and  $Eu^{3+}$  ions [3]. As the annealing temperature increased, the PL emission and excitation intensity increased and showed a maximum at 1200 °C. This was attributed to the improvement in the crystalline quality of the films. The PL emission and excitation intensity decreased at 1300 °C which was due to the formation of  $Y_2SiO_5$  phase by the reaction of the film with the quartz substrate.

## Conclusions

Optically transparent  $Y_2O_3:Eu$  films were deposited on fused quartz substrates by RF magnetron sputtering. We have shown that the optical transparency, crystalline quality, and luminescent characteristics of the  $Y_2O_3:Eu$



**Fig. 4.** AFM images of the  $\text{Y}_2\text{O}_3:\text{Eu}$  films (a) as-deposited and annealed at (b) 1000 °C, (c) 1100 °C, (d) 1200 °C, and (e) 1300 °C.

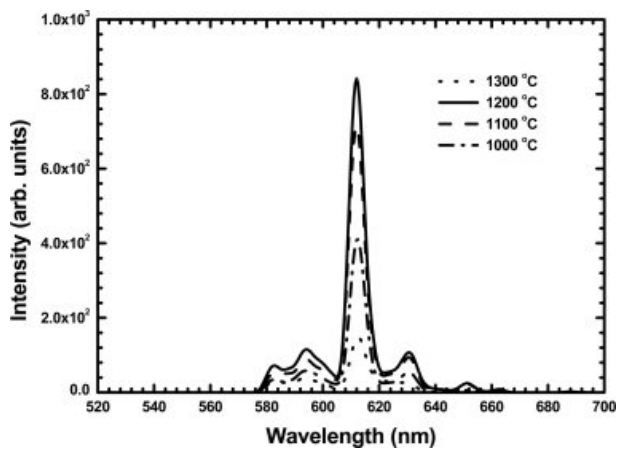


**Fig. 5.** Photoluminescence emission spectra of the  $\text{Y}_2\text{O}_3:\text{Eu}$  films annealed at different temperatures.

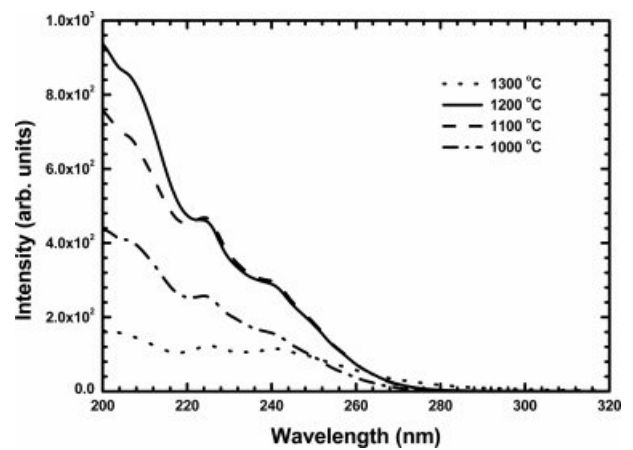


**Fig. 6.** PL excitation spectra of the  $\text{Y}_2\text{O}_3:\text{Eu}$  films annealed at different temperatures.

films were strongly affected by the thermal annealing treatment. The as-deposited  $Y_2O_3:Eu$  films showed a transparency of 89% at 550 nm and an optical band gap of 5.78 eV. The transparency and optical band gap of the films were found to decrease with increasing annealing temperature. XRD analysis revealed that the crystalline quality of the films was significantly improved by the thermal annealing treatment. The annealed  $Y_2O_3:Eu$  films showed a PL emission with the highest emission peak near 612 nm. The PL intensity was increased with increasing annealing temperature due to the improvement in the crystalline quality of the films. The PL intensity decreased at 1300 °C resulting from the formation of  $Y_2SiO_5$  phase.

### Acknowledgments

This work was supported by the National Research Foundation of Korea (NRF) grant funded by the Korea government (MSIT) (No. 2019R1F1A1040480).

### References

1. W.-B. Pei, Z.-Y. Jing, L.-T. Ren, Y. Wang, J. Wu, L. Huang, R. Lau, and W. Huang, *Inorg. Chem.* 57[17] (2018) 10511-10517.
2. J. Janek, M. Soltys, L. Zur, E. Pietrasik, J. Pisarska, W.A. Pisarski, *Mater. Chem. Phys.* 180 (2016) 237-243.
3. G. Blasse and B.C. Grabmaier, in "Luminescent Materials" (Springer-Verlag, Berlin, Heidelberg, 1994) p. 25.
4. L. Ji, N. Chen, G. Du, M. Yan, and W. Shi, *Ceram. Inter.* 40 (2014) 3117-3122.
5. W. Cheng, F. Rechberger, and M. Niederberger, *ACS Nano* 10[2] (2016) 2467-2475.
6. W. Liu, Y. Wang, M. Zhang, and Y. Zheng, *Mater. Lett.* 96 (2013) 42-44.
7. D. Den Engelsen, P. Harris, T. Ireland, R. Withnall, and J. Silver, *ECS J. Solid State Sci. Technol.* 2[9] (2013) R201-R207.
8. W. Chen, M. Zhou, Y. Liu, S. Fu, Y. Liu, Y. Wang, Z. Li, Y. Li, Y. Li, and L. Yu, *J. Alloys Compd.* 656 (2016) 764-770.
9. J.A. Nelson, E.L. Brant, and M.J. Wagner, *Chem. Mater.* 15[3] (2003) 688-693.
10. Y. Shimomura and N. Kijima, *Electrochem. Solid-State Lett.* 7[2] (2004) H1-H4.
11. S.T. Mukherjee, V. Sudarsan, P.U. Sastry, A.K. Patra, and A.K. Tyagi, *J. Alloys Compd.* 519 (2012) 9-14.
12. X. Hou, S. Zhou, Y. Li, and W. Li, *J. Alloys Compd.* 494 (2010) 382-385.
13. P. H. Holloway, T. A. Trottier, B. Abrams, C. Kondoleon, S. L. Jones, J. S. Sebastian, and W. J. Thomes, *J. Vac. Sci. Technol. B* 17[2] (1999) 758-764.
14. D. Ghosh, P. Ghosh, T. Noda, Y. Hayashi, and M. Tanemura, *Phys. Status Solidi-R* 7[12] (2013) 1080-1083.
15. J. Tauc, in "Amorphous and Liquid Semiconductors" (Plenum, New York, 1974) p.159.
16. T. Das, C. Mahata, S. Mallik, S. Varma, G. Sutradhar, P. K. Bose, and C. K. Maiti, *J. Electrochem. Soc.* 159[3] (2012) H323-H328.
17. Joint Committee on Powder Diffraction Standards (JCPDS), Powder Diffraction Files, Inorganic, No. 43-1036.
18. Joint Committee on Powder Diffraction Standards (JCPDS), Powder Diffraction Files, Inorganic, No. 47-1274.
19. Joint Committee on Powder Diffraction Standards (JCPDS), Powder Diffraction Files, Inorganic, No. 36-1476.